Data-driven Rigid Motion Correction for Helical CT

Tao Sun, Jung-Ha Kim, Roger Fulton, Johan Nuyts

***Abstract*— Although current CT systems can scan the head in a very short time, patient motion sometimes still induces artifacts. If motion occurs, one has to repeat the scan; to avoid motion, sedation or anesthesia is sometimes applied. Previously, we demonstrated the feasibility of rigid motion correction for helical CT brain imaging, using an optical tracking system. This correction is effective, but small residual motion errors may remain because of the limited accuracy of the tracking system. In such case, 'jagged' artifacts are observed in the reconstruction of a Hoffman phantom after the motion correction. We propose a data-driven method to iteratively correct this residual motion. In every iteration, we estimate the motion view-by-view, which then can be used to update the system matrix used during reconstruction. The evaluation on a phantom measurement showed that the reconstructed image improved as the iteration number increased.**

***Index Terms*—Computer Tomography (CT), iterative reconstruction, rigid motion, data-driven correction.**

I. INTRODUCTION

Assessment of the subject motion is of considerable general interest in tomography. A variety of methods for the estimation of motion in CT exist, including direct motion estimation using a camera system with visual markers [1]–[4] or without markers [5]–[7]. Artificial or anatomical landmarks can be also tracked in the image or projection domain [8], [9]. Indirect estimation methods have been proposed where motion is estimated through the minimization of errors in consistency conditions using projection moments [10], [11], or by an iterative process using re-projected image information [12]–[14]. Another approach has used similarity measures to quantify changes between projections to measure subject motion [15].

Previously, our group has developed and optimized a rigid motion correction technique for helical CT brain scanning, which measures the head motion with a Polaris system (Spectra, Northern Digital Inc, Waterloo, Canada) [1], [2]. As shown in Fig. 1, some small irregularities were still visible at the edges of the phantom in the reconstruction image after motion correction. The possible reason is that there still is some residual unrecorded motion in each pose, caused by small errors in the pose measurements. This will result in 'jagged' artifacts which are most visible at the edge of the phantom. This work aims to reduce or eliminate these residual motion estimation errors, by further refining the motion estimates using the measured data only.

Manuscript received Jan. 16, 2015. This work was supported in part by the IWT MIRIAD SBO project.

T. Sun and J. Nuyts are with the Medical Imaging Research Center, Department of Nuclear Medicine, KU Leuven, Belgium.

J. Kim is with the Discipline of Medical Radiation Sciences, University of Sydney, Australia.

R. Fulton is with the Discipline of Medical Radiation Sciences, and School of Physics, University of Sydney, and the Department of Medical Physics, Westmead Hospital, Westmead, Australia.

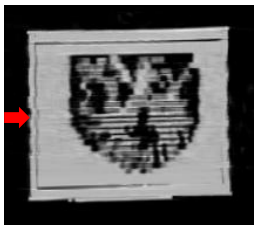

Fig. 1. Image after motion correction with measured poses with a pitch of 1.0. [Window Level=-200HU, Window Width=+2000HU]

II. METHOD

A. Motion estimation

Based on the previous work, it was assumed that most of the motion during the scan can be recorded by an external camera [1], [2]. Since the residual movement is relatively small after motion correction, the reconstruction should still be a reasonable estimate of the density distribution (Fig. 2). This little-corrupted estimate was used to calculate a set of 2-D projections that can be directly compared with the measured projections. Consequently, one can try to determine the 3-D orientation of the reconstructed object that produces the optimal match between calculated and measured projections. When this optimal orientation is determined, the motion estimate is updated and a new, improved reconstruction can be computed. Fig 2 gives a schematic description of the method, the following paragraphs describe in more details how the object orientation was estimated for each view.

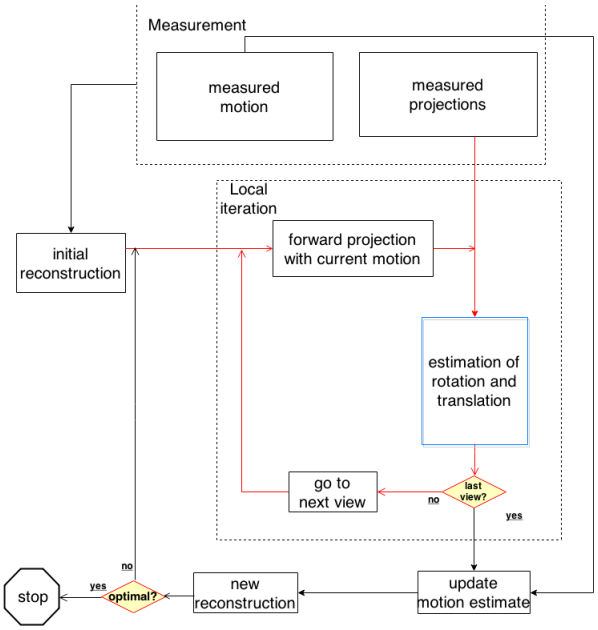

Fig. 2. General motion estimation and correction scheme.

A simple analytical relationship between the calculated and measured projection is derived by linearizing the problem, which is justified because we can assume that the residual motions are small. E.g., to estimate the residual rotation $\tilde{\alpha}$, a small rotation $\Delta\alpha$ is introduced to estimate the derivative of the projection with respect to the angle. For a 2D problem one obtains:

$$\frac{\partial P_{I,\theta}(\alpha,u_0,v_0)}{\partial\alpha} \approx \frac{P_{I,\theta}(\alpha_0+\tilde{\alpha},u_0,v_0)-P_{I,\theta}(\alpha_0,u_0,v_0)}{\tilde{\alpha}} \approx \frac{P_{I,\theta}(\alpha_0+\Delta\alpha,u_0,v_0)-P_{I,\theta}(\alpha_0,u_0,v_0)}{\Delta\alpha} \quad (1)$$

where $P_{I,\theta}$ is 1-dimensional forward projection at view θ of the image I, α_0 is the current rotation, u_0, v_0 are the current translations, $\tilde{\alpha}$ is the rotation to be estimated, $\Delta\alpha$ is a known small rotation (typically 0.5 degrees). We use the measured projection for $P_{I,\theta}(\alpha_0+\tilde{\alpha},u_0,v_0)$, $P_{I,\theta}(\alpha_0,u_0,v_0)$ is the forward projection of the current image I and $P_{I,\theta}(\alpha_0+\Delta\alpha,u_0,v_0)$ is computed by forward projection of a rotated version of that image. Then $\tilde{\alpha}$ is estimated as

$$\tilde{\alpha} = \arg\min_t \left(\sum_i \left(\Delta P(i) - t\cdot\Delta P_0(i) \right)^2 \right) \cdot \Delta\alpha \quad (2)$$

where

$$\Delta P = P_{I,\theta}(\alpha_0+\tilde{\alpha},u_0,v_0)-P_{I,\theta}(\alpha_0,u_0,v_0),$$
$$\Delta P_0 = P_{I,\theta}(\alpha_0+\Delta\alpha,u_0,v_0)-P_{I,\theta}(\alpha_0,u_0,v_0) \quad (3)$$

A similar approach was applied to estimate the translation parallel to the detector, except that the measured projection was simply shifted to (approximately) model the effect of a small known translation, avoiding the need for an additional projection. The effect of a small translation towards the source produces a very small magnification [16], which was found to have a negligible effect on the final reconstruction. Therefore, this translation was not estimated.

Extension to 3-D is straightforward, where 3 rotations and 2 translations have to be estimated. We found that it is beneficial to estimate the translations only in the very first iteration. The reason is that the translations are usually easier to estimate, compared to rotations [16], [17]. Using the translation-corrected reconstruction will give a reasonable input for the subsequent estimations. Another concern is the CT scanner used for the phantom measurements is a 16-slice system. The thin z-coverage in each view makes it extremely difficult to estimate the coronal and sagittal rotations if the translation is not correct. In the second iteration only the rotations are estimated, in all subsequent iterations both the rotations and translations were estimated.

After estimating the residual motions for all views, the motion estimate is updated and a new reconstruction (taking into account the updated motion) is computed using an iterative reconstruction algorithm. This new reconstruction is then used as the input for the next iteration. The whole iterative process was stopped, either if the projection errors were small enough or if the residual artifacts in the image were judged to be negligible.

B. Real scan experiment

The 3D Hoffman brain phantom, which contained air inside (instead of the usual water) was used in the experiments. The experiment was performed in the Department of Nuclear Medicine and Ultrasound at Westmead Hospital, on a Siemens Somatom Sensation 16 (Siemens Medical Solutions USA, Knoxville, TN). Some parameters of the spiral-CT scanner are listed below: pitch 1.0; tube voltage 120 kVp; tube current 150 mAs; rotation time 0.5 second; angles per rotation 1160; collimation 16×0.75 mm.

An optical motion tracking system (Polaris Spectra, Northern Digital, Waterloo, Canada) was placed at the rear of the scanner (Fig. 3). The phantom was placed off-center on the curved bed and held in place with a wedge. During the scan, the wedge was removed by pulling a string from outside the room. The phantom then started rolling left and right on the bed to finally come at rest at a stable position at the center of the bed. The 6 degrees of freedom of the motion of the phantom are shown in Fig. 4 relative to its pose at the start of the scan. The figure illustrates the oscillatory nature of the motion, including rotations of at least 10^0 about all axes, and translations of up to 103 mm.

We used a maximum likelihood reconstruction algorithm for transmission tomography (MLTR) with motion correction [1], [18] as the reconstruction algorithm. We ran 6 iterations for each reconstruction, while the number of subsets was selected as 80. The bed projections were subtracted from the measured projections beforehand. Reconstruction voxel size was $1.5\times1.5\times1.5$ mm. The (back)projector ray tracing used the Joseph interpolation [19]. To accelerate the calculations adjacent detectors were averaged and treated as a single larger detector, reducing the number of sinogram columns by a factor 2, and the reconstructed image was reduced to reduce the number of zero background pixels that had to be reconstructed. The object was centered in the reconstructed space for every new reconstruction.

For 3D helical CT, the first and last slices of the reconstructed image may suffer from artifacts due to the long object problem. To avoid this, the helical scan covered a bit more than the entire object and no motion was estimated for the first and last 10 planes.

Fig. 3. Motion tracking setup for a CT on a Siemens Biograph 16 PET/CT scanner. This figure is from [20].

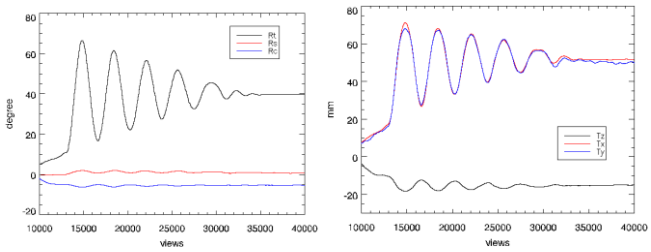

Fig. 4. Rotation and translation of the recorded oscillatory motion.

The motion estimates were median filtered (by median filtering each component independently) to remove outliers. We attribute the presence of these outliers to the small axial field of view of the CT detector (16 slices), which may cause errors in estimating the axial translation. Such an error in turn adversely affects the estimates of the other components of the motion.

III. Results

The motion estimation was done for 6 global-iterations. We did not run too many iterations because the visual improvement was almost invisible after 6 iterations, and the reconstruction time per iteration of our non-optimized research code is rather long (~6 hrs). Also, because of the high rotation speed, we estimated the motion every 4th projection view, followed by a linear interpolation between those views. The recovered motion and image are shown in Fig. 5, and Fig. 6 respectively. The image quality is significantly improved compared to the image before correction for residual motion: sharper resolution in transaxial view, less artifacts in coronal and sagittal views. A decreasing trend in projection error with increasing iteration number can be seen in Fig. 7.

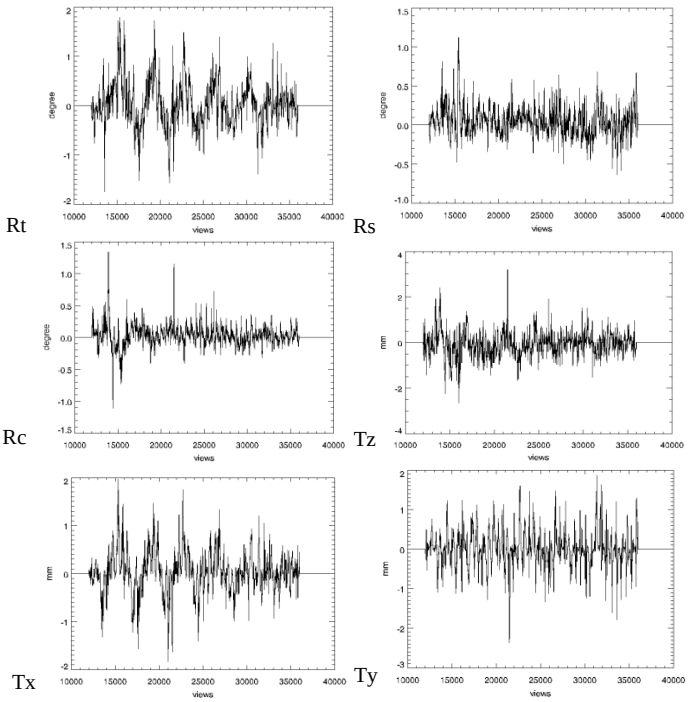

Fig. 5. Recovered residual motion after 6 global-iterations.

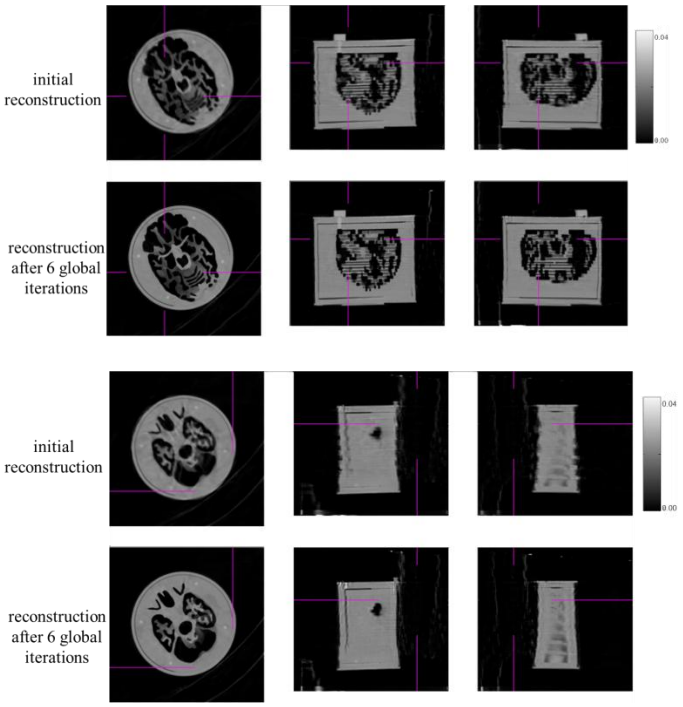

Fig. 6. Selected transaxial, sagittal and coronal planes, before and after correction for residual motion.

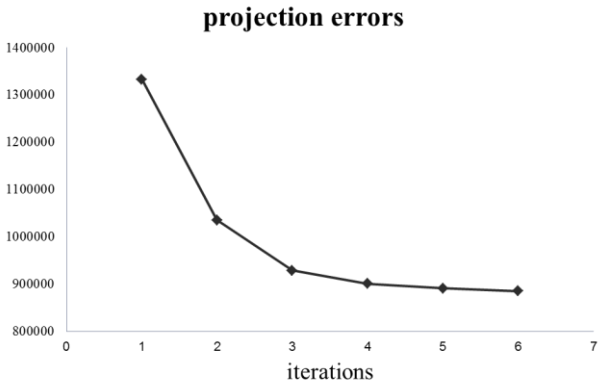

Fig. 7. Absolute value of the difference between measured and updated projections, as the global-iteration number increases.

IV. Conclusion

The phantom experiment was performed with a 16 slice CT, while most of the clinical CT scanners nowadays have more detector rows. Simulations with 40-slice and 128-slice CT are currently ongoing. The performance is expected to improve for a higher number of detector rows.

We have not shown any simulation results from motion estimation under noisy projection conditions. Although the real data study has confirmed the noise tolerance of the proposed method to some extent, a more rigorous analysis of the effect of noise on the image recovery is required.

The computation time is fairly important when translating a data-driven motion correction technique into clinics. The vast number of CT views in clinical scans results in a huge computing load. The rough time per iteration in our real data study was 6 hours for reconstruction and 1 hour for motion

estimation. To accelerate the reconstruction, we reconstructed a region-of-interest instead of the full FOV, and we rebinned the detectors with a factor of 2. Further acceleration will be necessary, e.g. by developing an OpenCL implementation to obtain parallel processing on GPU and/or CPU.

In both 3D simulation and real data studies, we used the assumption that the motion consists of a large measured motion and a small unknown motion. This matches the objective that we want to eliminate the residual motion which remains after the motion correction based on optical motion tracking. However, most of the motion during the CT scan will not be as dramatic as in Fig. 4. The proposed method can be directly used when the motion during the scan is relatively small across all the views. Evaluation of the performance of the method for larger motions is ongoing.

REFERENCES

[1] J. Nuyts, J.-H. Kim, and R. Fulton, "Iterative CT reconstruction with correction for known rigid motion," *11th Int. Meet. Fully 3D Reconstr. Radiol. Nucl. Med.*, pp. 132–135, 2011.

[2] J.-H. Kim, J. Nuyts, Z. Kuncic, and R. Fulton, "The feasibility of head motion tracking in helical CT: a step toward motion correction.," *Med. Phys.*, vol. 40, no. 4, p. 41903, Apr. 2013.

[3] A. Kyme, V. Zhou, S. Meikle, and R. Fulton, "Real-time 3D motion tracking for small animal brain PET.," *Phys. Med. Biol.*, vol. 53, no. 10, pp. 2651–66, May 2008.

[4] U. K. Bhowmik and R. R. Adhami, "A head motion measurement system suitable for 3D cone-beam tomography using markers," in *2012 IEEE Eng. Med. Biol. Soc. Conf. Proc.*, 2012, pp. 5975–5978.

[5] P. J. Noonan, J. Howard, T. F. Cootes, W. A. Hallett, and R. Hinz, "Realtime markerless rigid body head motion tracking using the Microsoft Kinect," in *2012 IEEE Nucl. Sci. Symp. and Med. Imag. Conf. Rec.*, 2012, pp. 2241–2246.

[6] O. V. Olesen, J. M. Sullivan, T. Mulnix, R. R. Paulsen, L. Hojgaard, B. Roed, R. E. Carson, E. D. Morris, and R. Larsen, "List-Mode PET Motion Correction Using Markerless Head Tracking: Proof-of-Concept With Scans of Human Subject," *IEEE Trans. Med. Imaging*, vol. 32, no. 2, pp. 200–209, 2013.

[7] A. Kyme, S. Se, S. Meikle, G. Angelis, W. Ryder, K. Popovich, D. Yatigammana, and R. Fulton, "Markerless Motion Tracking of Awake Animals in Positron Emission Tomography.," *IEEE Trans. Med. Imaging*, vol. 33, no. 11, pp. 2180–2190, Jun. 2014.

[8] W. Lu and T. R. Mackie, "Tomographic motion detection and correction directly in sinogram space," *Phys. Med. Biol.*, vol. 47, no. 8, pp. 1267–1284, Apr. 2002.

[9] C. J. Ritchie, C. R. Crawford, J. D. Godwin, K. F. King, and Y. Kim, "Correction of Computed Tomography Motion Artifacts Using Pixel-Specific Back-Projection," *IEEE Trans. Med. Imaging*, vol. 15, no. 3, pp. 333–342, 1996.

[10] H. Yu and G. Wang, "Motion Artifact Reduction in Fan-Beam CT," *IEEE Trans. Med. Imaging*, vol. 26, no. 2, pp. 249–260, 2007.

[11] H. Yu, Y. Wei, J. Hsieh, and G. Wang, "Data Consistency Based Translational Motion Artifact Reduction in Fan-Beam CT," *IEEE Trans. Med. Imaging*, vol. 25, no. 6, pp. 792–803, 2006.

[12] B. F. Hutton, S. Member, A. Z. Kyme, Y. H. Lau, D. W. Skerrett, and R. R. Fulton, "A Hybrid 3-D Reconstruction / Registration Algorithm for Correction of Head Motion in Emission Tomography," *IEEE Trans. Nucl. Sci.*, vol. 49, no. 1, pp. 188–194, 2002.

[13] Y. Kyriakou, R. M. Lapp, L. Hillebrand, D. Ertel, and W. a Kalender, "Simultaneous misalignment correction for approximate circular cone-beam computed tomography.," *Phys. Med. Biol.*, vol. 53, no. 22, pp. 6267–6289, Nov. 2008.

[14] A. Kingston, A. Sakellariou, T. Varslot, G. Myers, and A. Sheppard, "Reliable automatic alignment of tomographic projection data by passive auto-focus.," *Med. Phys.*, vol. 38, no. 9, pp. 4934–4945, Sep. 2011.

[15] S. Ens, J. Ulrici, E. Hell, and T. M. Buzug, "Automatic motion correction in cone-beam computed tomography," in *2010 IEEE Nucl. Sci. Symp. and Med. Imag. Conf. Rec.*, 2010, pp. 3248–3251.

[16] G. T. Gullberg, B. M. W. Tsui, C. R. Craford, B. J.Glen, and J. T. Hagius, "Estimation of Geometrical Parameters for Cone Beam Tomography," *Med. Phys.*, vol. 17, no. 2, pp. 264–272, 1989.

[17] V. Patel, R. N. Chityala, K. R. Hoffmann, C. N. Ionita, D. R. Bednarek, and S. Rudin, "Self-calibration of a cone-beam micro-CT system," *Med. Phys.*, vol. 36, no. 1, p. 48, 2009.

[18] J. Nuyts, B. De Man, P. Dupont, M. Defrise, P. Suetens, and L. Mortelmans, "Iterative reconstruction for helical CT: a simulation study.," *Phys. Med. Biol.*, vol. 43, no. 4, pp. 729–737, Apr. 1998.

[19] P. M. Joseph, "An Improved Algorithm for Reprojecting Rays Through Pixel Images," *IEEE Trans. Med. Imaging*, vol. 1, no. 3, pp. 143–146, 1983.

[20] J.-H. Kim, J. Nuyts, A. Kyme, Z. Kuncic, and R. Fulton, "A rigid motion correction method for helical computed tomography (CT)," *Phys. Med. Biol.*, In press.